Study of the fatigue behaviour of synthetic nodular cast irons at low and high frequency cyclic loading

Alan Vaško[1,*], *Juraj* Belan[1], *Eva* Tillová[1]

[1]University of Žilina, Faculty of Mechanical Engineering, Department of Materials Engineering, Univerzitná 8215/1, 010 26 Žilina, Slovakia

Abstract. The paper presents the results of low and high frequency fatigue tests carried out on nodular cast iron. The specimens of synthetic nodular cast irons from three different melts were studied in the high cycle fatigue region (from 10^5 to 10^8 cycles) using fatigue experimental equipments for low and high frequency cyclic loading. Low frequency fatigue tests were carried out at frequency $f \approx 120$ Hz using the fatigue experimental machine Zwick/Roell Amsler 150HFP 5100. High frequency fatigue tests were carried out at frequency $f \approx 20$ kHz using the ultrasonic fatigue testing device KAUP-ZU. Both of them were carried out at sinusoidal cyclic push-pull loading (stress ratio $R = -1$) at ambient temperature ($T \approx 20$ °C). The relationship $\sigma_a = f(N)$ and fatigue strengths were determined experimentally; mechanical properties, microstructures and fracture surfaces were investigated.

Keywords: nodular cast iron, fatigue test, low frequency fatigue, high frequency fatigue, fatigue fracture

1 Introduction

The majority of service interruptions and cracks at the present time is caused by fatigue processes, degradation of materials properties in long time service and influence of external environment. The most significant of them is the failure caused by mechanical fatigue. The importance of fatigue results especially from the economical point of view (costs for development of new materials, testing equipments, methods of testing of prototypes and final products etc.) and safety of people whose life also depends on working reliability of devices.

Various internal and external factors significantly influence the fatigue characteristics of materials. The structural state of material and its chemical composition, grain size, shape and distribution of non-metallic inclusions, value of previous deformation etc. belong to the inside (internal) factors. The frequency of loading and load ratio, value of mean stress, state of stress, environment agresivity and temperature, history of loading, thickness and size of body, existence of apriory cracks, notches and other geometrical discontinuities, properties of surface layer etc. belong to outside (external) factors [1].

* Corresponding author: alan.vasko@fstroj.uniza.sk

Reviewers: *Darina* Ondrušová, *Františka* Pešlová

Although fatigue has been studied intensively over many years and many scientific papers and books were published, further study is necessary because the knowledge base is partly obsolete and new materials and treatments are continuously being developed [2]. Therefore the paper deals with the study of the fatigue behaviour of synthetic nodular cast irons at low and high frequency cyclic loading.

Nodular cast iron is a group of cast structural materials with a wide application in engineering practice (especially in the automotive industry). It combines high tensile strength and plasticity with high fatigue strength.

Nodular cast iron can be produced according to the classical or synthetic casting procedure (Fig. 1) which is more economical [3]. Classical melts use pig iron as a basic charging raw material. Nowadays, the production of nodular cast iron has been from an economic point of view orientated to synthetic melts where a part of more expensive pig iron in a metal charge is substituted for cheaper steel scrap. The transition from the traditional use of pig iron to synthetic nodular cast iron prepared from steel scrap requires the regulation of chemical composition of melt. Steel scrap has low content of silicon therefore increasing of content of silicon to eutectic composition ($S_C \approx 1$) is reached by using of ferrosilicon (FeSi) or metallurgical silicon carbide (SiC) additive. Addition of metallurgical SiC to a nodular cast iron melt shows specific advantages in comparison with other Si and C carriers what has been described as a special pre-inoculating effect [4-7].

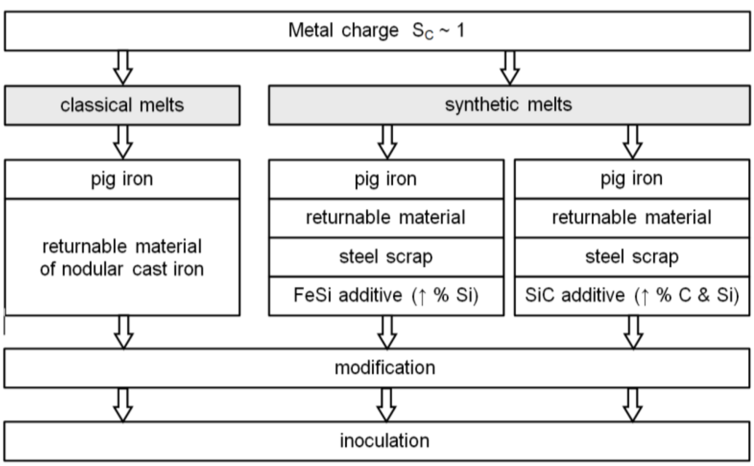

Fig. 1. Scheme of the production of nodular cast iron

2 Experimental material and methods

Three different melts of nodular cast iron were chosen for experiments and the specimens from them were used for metallographic analysis, mechanical tests, fatigue tests and microfractographic analysis. Similar chemical composition of the melts was achieved by different charge composition (Table 1). The basic charge of individual melts consisted of pig iron, steel scrap and some additives for the regulation of chemical composition. The content of these additives was chosen to achieve similar resultant chemical composition of the melts (eutectic degree $S_C \approx 1.2$).

The basic charge of the melt 1 was formed by 40 % of pig iron and 60 % of steel scrap with the additives of carburizer and metallurgical silicon carbide SiC90. The basic charge of the melt 2 was formed only by steel scrap (it did not contain any pig iron) with the same additives for the regulation of chemical composition (carburizer and silicon carbide SiC90).

The basic charge of the melt 3 was also formed by 40 % of pig iron and 60 % of steel scrap but there were used different additives for the regulation of chemical composition (carburizer and ferrosilicon FeSi75). Modifier FeSiMg7 and inoculant FeSi75 were used in the same amount for all the melts.

Table 1. Charge composition of experimental melts

Melt number	**Pig iron (%)**	**Steel scrap (%)**	**Additives**	**Modifier & inoculant**
1	40	60	carburizer + SiC90	FeSiMg7 + FeSi75
2	0	100	carburizer + SiC90	
3	40	60	carburizer + FeSi75	

Experimental bars of diameter 32 mm and length 350 mm were cast from all the melts and consequently specimens for metallographic analysis, tensile test, impact bending test, hardness test and fatigue tests were made.

The metallographic analysis of specimens from experimental melts was made by the light metallographic microscope Neophot 32. The specimens for metallographic analysis were taken out from the cast bars and prepared by usual metallographic procedure. The microstructure of specimens was evaluated according to STN EN ISO 945 and by automatical image analysis [8, 9]. The image analysis system NIS Elements, interfaced with the light microscope, was used for the evaluation of shape factor, count of graphitic nodules per unit of area and content of ferrite in the matrix. The final value is the average of at least 10 measurements, each at different place of the specimen.

The tensile test was carried out according to STN EN ISO 6892-1 by means of the testing equipment ZDM 30 with a loading range F = 0 to 50 kN. The impact bending test was carried out according to STN EN ISO 148-1 by means of the Charpy hammer PSW 300 with a nominal energy of 300 J. The Brinell hardness test was carried out according to STN EN ISO 6506-1 by means of the testing equipment CV-3000 LDB with a hardmetal ball of diameter D = 10 mm forced into specimens under the load F = 29 430 N (3000 kp) [10, 11].

The fatigue tests were carried out according to STN 42 0362 at low and high frequency sinusoidal cyclic push-pull loading (stress ratio R = -1) at ambient temperature (T = 20 ± 5 °C). Low frequency fatigue tests were carried out at frequency $f \approx$ 120 Hz using the fatigue experimental machine Zwick/Roell Amsler 150HFP 5100 (Fig. 2). High frequency fatigue tests were carried out at frequency $f \approx$ 20 kHz using the ultrasonic fatigue testing device KAUP-ZU (Fig. 3) [12, 13].

Test specimens of circular cross-section were used for fatigue tests. Shape and parameters of the specimens for low frequency cyclic loading are shown in Fig. 2c and for high frequency cyclic loading in Fig. 3c. For both fatigue tests, ten specimens from each melt were used to obtain the relationship between the applied amplitude of cyclic stress and the number of cycles to failure (Wöhler curve) and to determine the fatigue strength [14].

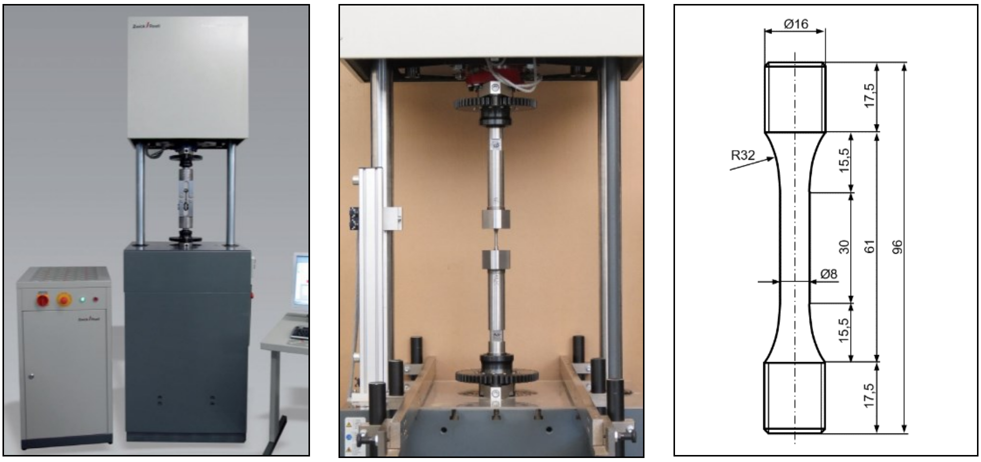

a) fatigue experimental machine Zwick/Roell Amsler 150HFP 5100 b) detail of fatigue testing c) shape and parameters of the test specimens

Fig. 2. Experimental device and specimen for low frequency fatigue test

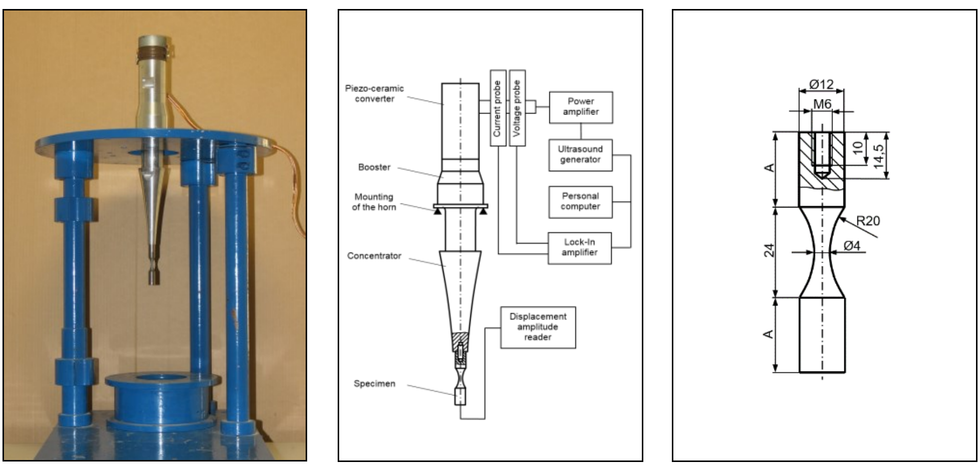

a) ultrasonic fatigue testing device KAUP-ZU b) scheme of testing apparatus c) shape and parameters of the test specimens

Fig. 3. Experimental device and specimen for high frequency fatigue test

The microfractographic analysis of fracture surfaces is an inseparable part of every work in the field of fatigue. Fracture surfaces of the specimens fractured by fatigue tests were investigated by the scanning electron microscope VEGA II LMU [15].

3 Experimental results and discussion

3.1 Metallographic analysis

Microstructure of the specimens from experimental melts is shown in Fig. 4. All the specimens are ferrite-pearlitic nodular cast irons with similar content of ferrite and pearlite in the matrix, similar shape, size and count of graphitic nodules (Table 2). Differences in the microstructure of individual specimens are caused by different ratio of pig iron and steel scrap in the charge and by different kind of additive for the regulation of the chemical composition (SiC or FeSi).

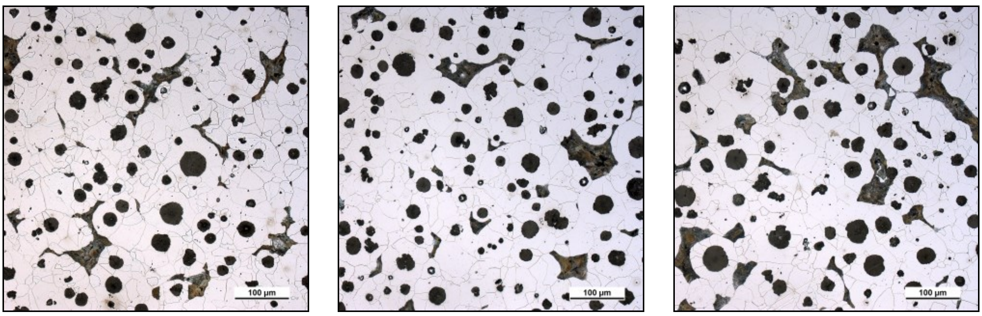

a) melt 1 b) melt 2 c) melt 3

Fig. 4. Microstructure of the specimens from cast bars, etched by 1% Nital

The results of evaluation of the microstructure according to STN EN ISO 945 and by image analysis (shape factor, count of graphitic nodules and content of ferrite) are presented in Table 2. The microstructural parameters evaluated in the specimens from the melts with SiC additive are higher than in the specimens from the melt with FeSi additive. The highest content of ferrite (approximately 78%) was reached in the melt 2, formed only by steel scrap with SiC additive and in the melt 1, formed by 40 % of pig iron and 60 % of steel scrap with SiC additive. Graphite occurs only in a perfectly-nodular and imperfectly-nodular shape in all the specimens. The size of graphite is from 30 to 120 μm, but in all the specimens the size within 30-60 μm predominates. The highest ratio of perfectly-nodular graphite (80 %), the highest shape factor (0.83) and the highest count of graphitic nodules per unit of area (almost 200 mm^{-2}) were reached in the melt 1, formed by 40 % of pig iron and 60 % of steel scrap with SiC additive.

Table 2. Results of evaluation of the microstructure

Melt number	**STN EN ISO 945**	**Shape factor ***	**Count of graphitic nodules (mm^{-2})**	**Content of ferrite (%)**
1	80%VI5/6 + 20%V6	0.83	199.8	74.0
2	70%VI5/6 + 30%V6	0.82	179.8	78.0
3	70%VI5/6 + 30%V6	0.79	151.0	65.2

* $S = 4\pi A/P^2$ (*A* – area of an graphitic nodule, *P* – perimeter of an graphitic nodule)

3.2 Mechanical tests

Mechanical properties (tensile strength R_m, elongation A, absorbed energy $K0$ and Brinell hardness HBW) of the specimens from experimental melts are summarised in Table 3.

Table 3. Mechanical properties of the specimens

Melt number	R_m (MPa)	A (%)	K0 (J)	HBW 10/3000
1	539.0	4.0	30.6	192.3
2	515.7	3.7	17.2	182.3
3	462.6	2.7	24.0	181.3

The specimens from the melts with SiC additive have better mechanical properties than the specimens from the melt with FeSi additive. It has connection with the microstructure of the specimens, especially with the character of matrix (content of ferrite and pearlite) and also with the shape, size and count of graphitic nodules. The best mechanical properties were reached in the melt 1, formed by 40% of pig iron and 60% of steel scrap with SiC additive, which has the highest ratio of perfectly-nodular graphite, the highest shape factor, the highest count of graphitic nodules and the smallest size of graphite.

3.3 Fatigue tests

For fatigue tests, ten specimens from each melt were used to obtain Wöhler fatigue curves $\sigma_a = f(N)$ and determine fatigue strength σ_c for $N = 10^7$ cycles (in the case of low frequency cyclic loading) or σ_c for $N = 10^8$ cycles (in the case of high frequency cyclic loading).

The results of fatigue tests (relationship between stress amplitude σ_a and number of cycles to failure N_f) obtained at low frequency cyclic loading ($f \approx 120$ Hz) are shown in Fig. 5a. The number of cycles to failure increases with a decreasing stress amplitude.

The values of fatigue strength σ_c determined for $N = 10^7$ cycles in comparison with tensile strength R_m are given in Table 4. The fatigue strength in analysed specimens of nodular cast iron increases with an increasing tensile strength. The fatigue strength in the specimens from the melts with SiC additive is higher than in the specimens from the melt with FeSi additive. The highest fatigue strength (255 MPa) was reached in the melt 1, formed by 40% of pig iron and 60% of steel scrap with SiC additive, which also has the best mechanical properties.

The results of fatigue tests obtained at high frequency cyclic loading ($f \approx 20$ kHz) are shown in Fig. 5b. The number of cycles to failure also increases with decreasing stress amplitude.

The values of fatigue strength σ_c determined for $N = 10^8$ cycles in comparison with tensile strength R_m are given in Table 4. At higher values of tensile strength there was observed an increase in fatigue strength. The highest fatigue strength (218 MPa) was reached in the melt 1, formed by 40% of pig iron and 60% of steel scrap with SiC additive, similarly to low frequency cyclic loading.

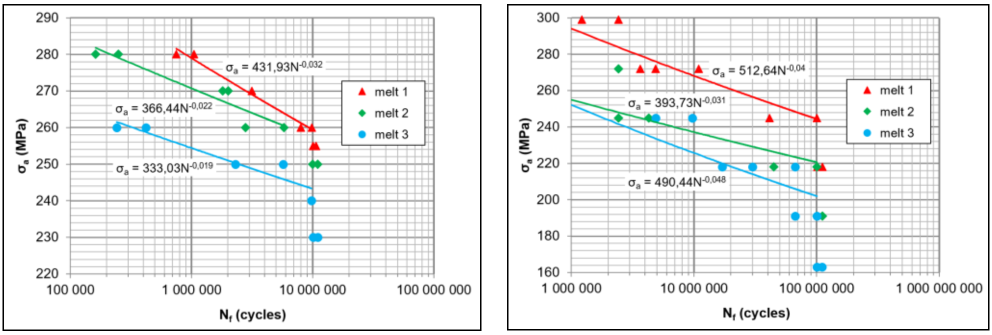

a) low frequency cyclic loading ($f \approx 120$ Hz) b) high frequency cyclic loading ($f \approx 20$ kHz)

Fig. 5. Wöhler curves $\sigma_a = f(N)$

Table 4. Comparison of tensile strength R_m and fatigue strength σ_c for low frequency cyclic loading (LFCL) and high frequency cyclic loading (HFCL)

Loading/ frequency		**LFCL f ≈ 120 Hz**	**HFCL f ≈ 20 kHz**	
Melt number	**R_m (MPa)**	**σ_c (MPa) for N = 10^7 cycles**	**σ_c (MPa) for N = 10^8 cycles**	**$\sigma_{c\,10^7}$ (MPa)** (calculated)
1	539.0	255	218	268
2	515.7	250	191	237
3	462.6	230	163	226

The values of fatigue strength σ_c for $N = 10^7$ cycles obtained at low frequency cyclic loading are in a good agreement with the values of fatigue strength σ_c for $N = 10^8$ cycles obtained at high frequency cyclic loading as well as the values of timing fatigue strength $\sigma_{c\,10^7}$ calculated for $N = 10^7$ cycles.

3.4 Microfractographic analysis

The fracture surfaces of analysed specimens after fatigue failure do not show any remarkable differences; they are characteristic of mixed mode of fracture. Examples of failure micromechanisms of the specimens at low and high frequency cyclic loading are documented in Fig. 6 and 7.

Fig. 6 shows the fracture surface of the specimen after low frequency cyclic loading with stress amplitude σ_a = 270 MPa and number of cycles to failure $N_f = 3.2 \times 10^6$. The fatigue fracture was initiated by casting defect. The fatigue fracture is characteristic of intercrystalline fatigue failure of ferrite around graphitic nodules and transcrystalline fatigue failure of ferrite and pearlite in the rest of the area (Fig. 6a). The final rupture is characteristic of transcrystalline ductile failure of ferrite with dimple morphology (Fig. 6b) and transcrystalline cleavage of ferrite and pearlite with river drawing on facets (Fig. 6c).

Fig. 7 shows the fracture surface of the specimen after high frequency cyclic loading with stress amplitude σ_a = 272 MPa and number of cycles to failure $N_f = 2.4 \times 10^6$. The fatigue failure of the specimen after high frequency cyclic loading has a mixed character of fracture, similarly to low frequency cyclic loading. The fatigue fracture is characteristic of intercrystalline fatigue failure of ferrite around graphitic nodules and transcrystalline fatigue failure of ferrite and pearlite in the rest of the area (Fig. 7a). The final rupture is characteristic of transcrystalline ductile failure of ferrite (Fig. 7b) and transcrystalline cleavage of ferrite and pearlite (Fig. 7c).

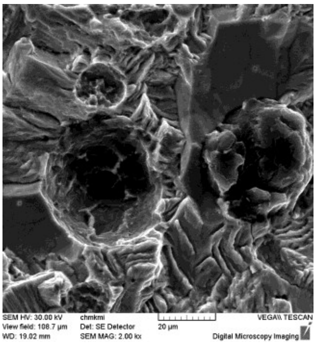

a) inter- and transcrystalline fatigue failure

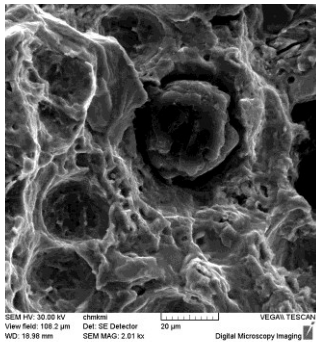

b) transcrystalline ductile failure

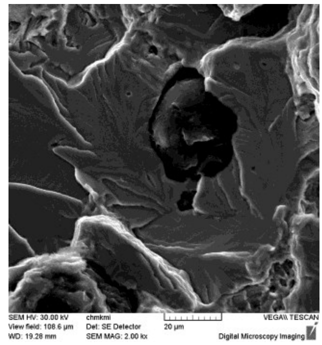

c) transcrystalline cleavage

Fig. 6. Failure micromechanisms of the specimen at low frequency cyclic loading (melt 1, $f \approx 120$ Hz, $\sigma_a = 270$ MPa, $N_f = 3.2 \times 10^6$ cycles), SEM

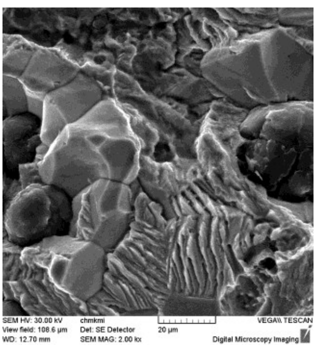

a) inter- and transcrystalline fatigue failure

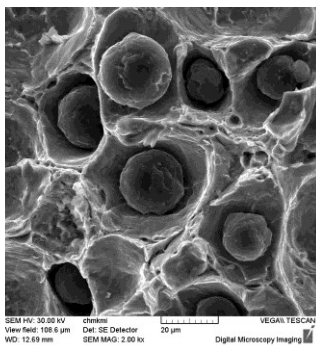

b) transcrystalline ductile failure

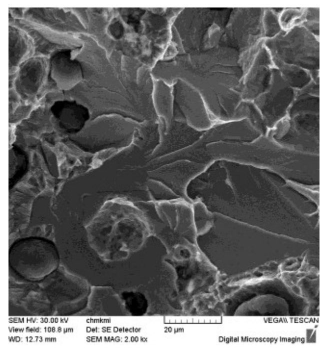

c) transcrystalline cleavage

Fig. 7. Failure micromechanisms of the specimen at high frequency cyclic loading (melt 2, $f \approx 20$ kHz, $\sigma_a = 272$ MPa, $N_f = 2.4 \times 10^6$ cycles), SEM

Conclusions

The experimental results can be summarized to the following points:

- The substitution of a part of pig iron for steel scrap in the charge together with SiC additive positively influences the microstructure of nodular cast iron and consequently the mechanical and fatigue properties are improved;
- The highest microstructural parameters (ratio of perfectly-nodular graphite, shape factor, count of graphitic nodules and content of ferrite) were reached in the specimen from the melt 1, formed by 40 % of pig iron and 60 % of steel scrap with SiC additive;
- The best mechanical properties (tensile strength, elongation, absorbed energy and Brinell hardness) as well as fatigue properties (fatigue strength for low and high frequency cyclic loading) were also reached in the specimens from the melt 1, formed by 40 % of pig iron and 60 % of steel scrap with SiC additive;
- The values of fatigue strength obtained at high frequency cyclic loading are in a good agreement with the results obtained at low frequency cyclic loading. Moreover, application of high frequency cyclic loading is characteristic with the significant time, energy and work saving;

- No significant differences were observed by the comparison of fracture surfaces of the specimens from the analysed melts. The fatigue failure has a mixed character of fracture in all the specimens; the intercrystalline fatigue failure predominates near graphitic nodules and the transcrystalline fatigue failure predominates in the rest of the area.

This work has been supported by the Scientific Grant Agency of Ministry of Education, Science, Research and Sport of Slovak Republic, grant project VEGA No. 1/0533/15 and by the Culture and Educational Grant Agency of Ministry of Education, Science, Research and Sport of Slovak Republic, grant project KEGA No. 049ŽU-4/2017.

References

1. L. Várkoly, J. Zuidema, B. Várkolyová, M. Chalupová, *Fatigue failure of materials – theory and solved examples*. (EDIS, Žilina, 1998)
2. O. Bokůvka, G. Nicoletto, M. Guagliano, L. Kunz, P. Palček, F. Nový, M. Chalupová, *Fatigue of materials at low and high frequency loading*. (EDIS, Žilina, 2014)
3. R. Konečná, M. Kokavec, G. Nicoletto, *Surface conditions and the fatigue behavior of nodular cast iron*. Procedia Engineering **10**, 2538-2543 (2011)
4. T. Benecke, S. Venkateswaran, W.D. Schubert, B. Lux, *Investigation of the influence of silicon carbide in the production of ductile cast iron*. Foundryman **87**, 355-360 (1994)
5. K. W. Copi, Y. S. Lerner, N. S. Laukhin, *SiC vs. 75% FeSi: Comparing pre-inoculation effects*. Modern Casting **93**, 29-31 (2003)
6. W. H. Zhang, J. Ding, F. R. Nie, *SiC inoculation pretreatment of cast iron*. Foundry (Zhuzao) **58**, 279-281 (2009)
7. A. Vaško, *Influence of SiC additive on microstructure and mechanical properties of nodular cast iron*. Materials science (Medžiagotyra) **14**, 311-314 (2008)
8. P. Skočovský, A.Vaško, *Quantitative evaluation of structure of cast irons*. (EDIS, Žilina, 2007, in Slovak)
9. R. Konečná, S. Fintová, *Methods of structure study*. (EDIS, Žilina, 2014, in Slovak)
10. A. Vaško, P. Skočovský, *Properties and using of metal materials*. (EDIS, Žilina, 2014, in Slovak)
11. P. Kopas, M. Vaško, M. Handrik, *Computational modeling of the microplasticization state in the nodular cast iron*. Applied Mechanics and Materials **474**, 285-290 (2014)
12. L. Trško, O. Bokůvka, F. Nový, M. Guagliano, *Effect of severe shot peening on ultra-high-cycle fatigue of a low-alloy steel*. Materials and Design **57**, 103-113 (2014)
13. R. Ulewicz, P. Tomski, *The effect of high-frequencies loading on the fatigue cracking of nodular cast iron*. Metalurgija **56**, 33-36 (2017)
14. S. Věchet, J. Kohout, O. Bokůvka, *Fatigue properties of nodular cast iron*. (EDIS, Žilina, 2001, in Czech)
15. P. Palček, M. Chalupová, *Fractography and influence of the structure on character of the fracture*. Proceedings of Summer school of fatigue of materials. (EDIS, Žilina, 2006, in Slovak)